## Lyotropic liquid crystal guest-host material and anisotropic thin films for optical applications

Irina Kasianova[a]; Ellina Kharatyian[a]; Artur Geivandov[a]; Serguei Palto[ab]

[a] Crysoptix KK, Tokyo, Japan [b] Institute of Crystallography RAS, Moscow, Russia

## PLEASE SCROLL DOWN FOR ARTICLE

Taylor & Francis
Taylor & Francis Group

# Lyotropic liquid crystal guest–host material and anisotropic thin films for optical applications

Irina Kasianova[a], Ellina Kharatyian[a], Artur Geivandov[a]* and Serguei Palto[a,b]

*[a]Crysoptix KK, Tokyo, Japan; [b]Institute of Crystallography RAS, Moscow, Russia*

We propose a new approach for the production of thin film optical functional materials. The method is based on molecular design whereby two different types of lyotropic liquid crystals (LC), lyotropic LC based on columnar supramolecules and water-soluble rod-like polymer molecules are mixed. The resulting lyotropic guest–host system allows production of optical retardation films with tunable optical anisotropy controlled by composition of the guest–host system. Coatable retarders can be used in modern liquid crystal displays and TVs for optical compensation and enhancement of the LCD's performance.

**Keywords:** liquid crystal display; lyotropic liquid crystal; optical anisotropy; retarder; thin film

## 1. Introduction

Optically anisotropic materials are of crucial significance in modern optical applications. The well-known achievements in information display technologies are based on development of anisotropic optical films made of materials such as liquid crystals (LC) and different types of functional polymers [1]. The functional properties of these materials depend on their phase state. Symmetry of a particular bulk phase and its supramolecular structure define the macroscopic performance of a material – its optical, mechanical and other properties.

One example is thermotropic liquid crystals. Depending on temperature, thermotropic liquid crystals can be in different thermodynamically stable phase states. However, it is only for the nematic phase that a set of bulk properties (allowed by symmetry) supports their ubiquitous application in optics and information displays. Thermotropic liquid crystal materials of a single type of molecule typically show a very narrow temperature range for the nematic phase (just a few °C). The problem was solved by developing liquid crystal mixtures, which in many instances can also be named as 'guest–host systems' [2]. Due to the 'guest–host' approach, the thermotropic liquid crystal materials provide the nematic phase in a temperature range larger than 100°C.

Guest–host systems are well-known in supramolecular chemistry [3] and biology [4]. They are composed of two or more molecules or ions held together in unique structural relationships by forces other than those of full covalent bonds [4]. In liquid crystals, the phenomenon of dissolving and aligning of any molecule or a group of molecules such as dyes, impurities or even mesogenic molecules by a liquid crystal can be called a guest–host phenomenon [2]. The guest molecules couple to the anisotropic intermolecular interaction field of the liquid crystal, but can diffuse rather freely within the host. The essential feature is that a guest–host system is composed of a single material without phase separation.

In the present paper we introduce lyotropic liquid crystal (LLC) guest–host systems. While the thermotropic liquid crystals show the nematic phase in a particular temperature range, the lyotropic liquid crystal nematic phase exists in a certain range of concentrations of materials in solution. The ability of a material to form the nematic phase is very important for many reasons. For instance, the anisotropy of the viscous–elastic properties of the nematic phase allows fine alignment of the molecules on solid substrates by shear flow [5]. In this way the optically anisotropic thin solid films can be deposited onto different substrates.

The aim of this work is the development of guest–host LLC materials for optically anisotropic thin solid films with a controlled optical anisotropy. In order to control the optical anisotropy, we propose an approach based on a special type of the guest–host system consisting of two different types of components. Both of the components can be in the nematic phase at some concentrations in aqueous solutions. While the first component forms the nematic phase with negative optical anisotropy (due to plank-like stacking molecules), the nematic phase of the second one is created by polymer macromolecules and characterised by positive optical anisotropy. In the guest–host system (which must also be in the nematic phase), the superposition of the two components with different signs of optical anisotropy results in strong modification of the resultant dielectric tensor. Thus the principal

*Corresponding author. Email: artur.geivandov@crysoptix.com

refractive indices of the phase can be controlled by the concentrations of the components in the guest–host system.

Our task was to develop the material which provides the nematic phase in a wide range of component concentrations. These allow deposition of the well-aligned films, which can be either optically uniaxial or biaxial after they have been dried and become solid. In addition, three of the principal refractive indices are well controlled in a wide range by changing the component concentrations, which allows the creation of different types of retardation films for liquid crystal displays (LCDs).

In a typical LCD, the liquid crystal layer is placed between two polarisers. Off-axis contrast drop is one of the inherent drawbacks arising from the optical anisotropy of LC materials and a feature of the propagation of the light through crossed polarisers. For instance, at oblique viewing directions, the light leakage can appear through the crossed polarisers, which increases with increasing off-axis angle. Thus the light leakage caused by both LC optical anisotropy and polarisers should be suppressed. This problem of cumulative off-axis contrast ratio decrease is solved using phase retardation films produced from optically anisotropic materials. The appropriate retardation films provide a small colour shift and high off-axis contrast (contrast ratio at wide viewing angles) to the LCD.

Most of the phase retardation films used in modern LCD technology are produced by means of mechanical stretching of the extruded or casted polymers. Control of optical anisotropy is achieved by adjusting stretching parameters as well as by using special additives capable of increasing or suppressing the material anisotropy [6]. A polymer optical film, for instance, can be attached to a PVA (polyvinyl alcohol) polariser sandwiched between protective layers. On the other hand, retardation films can combine both optical compensation and protective functions. For example, polycyclo-olefins are used for the manufacture of optical films for optical compensation of vertical alignment (VA) [7] and in-plane switching (IPS) [8] LCD modes, while at the same time supplying protective function. However, polycyclo-olefin based films as well as other hydrophobic polymeric materials have a problem of adhesion to the hydrophilic PVA layer. Besides, even in the case of hydrophilic stretched films such as triacetylcellulose [5, 9], improving their performance is difficult due to limitations of the mechanical stretching process, especially for the manufacture of large screen displays.

Typically, optical grade stretched retardation films possess small optical anisotropy ($\Delta n = 0.001$–$0.005$).

The reason is that combined functions of retardation film and PVA polariser protection film are usually reached if the plastic film possesses mechanical strength achieved at certain thickness of about 50 $\mu$m. In addition, such film should have high optical quality (e.g. low haze value) and be easily used in a technological process. An alternative to such 'thick' retardation films is a thin coating realised on a plastic or a glass substrate and embedded into a conventional polariser or inside a LC cell, respectively.

There is a large group of coatable retarders based on cross-linkable thermotropic liquid crystals. The production of such films comprises coating of a melt or a solution onto a substrate. In the latter case, coating is followed by solvent evaporation. Additional alignment procedures are involved such as application of an electric field or using alignment layers produced by rubbing or photo-alignment. This process can be used to manufacture uniaxial optical layers with positive and negative optical anisotropy [10, 11], biaxial retarders for the successively coated layers [12, 13], and films with complex space distribution of the local optical axes (tilted and splayed) for optical compensation of twisted nematic (TN) LCD mode [14]. Photo-aligning and a phase retardation function could be combined into a single material [15]. Ultraviolet (UV) curable materials can be used for high-resolution patterned retarders for transflective LCDs [10, 16].

An alternative, simple and cost-effective method of producing optical films is coating of LLC solutions, where small molecules are capable of self-assembling in columnar supramolecules [17, 18]. These compounds are also known as chromonics [19] and consist of amphiphilic molecules with flat conjugated core and polar solubilising groups at the periphery. The self-assembly in aqueous solution is based on $\pi$–$\pi$ interaction between aromatic cores and on the hydrophobic effect. The rod-like supramolecules in aqueous solution form the nematic type of liquid crystalline state, where the axes of the supramolecules within one domain are aligned along some preferable direction. In the course of deposition of a liquid crystalline solution onto a substrate (coating), an external shear force is applied and all supramolecules become aligned along the shear force direction. Such shear flow alignment is well known in thermotropic LCs and can be explained by anisotropy of the viscous–elastic properties of the nematic phase. Other approaches can be used in order to align LLC, for instance coating of lyotropic liquid crystalline solution onto the photo-aligned layer [20]. Solvent evaporation fixes the ordered structure, leading to formation of a solid birefringent film with macroscopic optical anisotropy. The molecules in such films are usually packed with their

minimal polarisability axes along the coating direction corresponding to the minimal principal refractive index. As a result, the method allows the production of optical films in the range from uniaxial negative A-plates to biaxial $B_A$-plates [21, 22].

The present paper is organised as follows. First we describe chemical synthesis of compounds for the guest–host system, followed by the thin film coating technique. The classification of retardation films is then given. The obtained retardation coatings made of single components and their mixture were studied by means of optical microscopy and polarisation spectroscopy. The mechanism of retardation control by virtue of components ratio found experimentally is discussed with modelling. Further, the unique thermal and mechanical properties of new guest–host retarders are demonstrated. At the end of paper, the optical performance of new retardation coatings applied in modern LCDs is simulated.

## 2. Synthesis and film coating technique

The scheme of the synthesis of 4,4′-(5,5-dioxido-dibenzo[b,d]thiene-3,7-diyl)dibenzenesulphonic acid (referred to as *para*-quaterphenyl disulphosulphone, pQpdSS) is presented in Figure 1(a). The hydrocarbon core of *para*-quaterphenyl was obtained via the Ullmann reaction as described elsewhere [23, 24]. Polar sulphonic groups were introduced during a sulphonation reaction in the subsequent stage.

Poly(2,2′-disulphobenzidine terephthalamide) (PBDT) was synthesised via a heterophasic polycondensation reaction (Figure 1(b)). The procedure described in the literature [25] was modified to control the molecular weight of the polymer precisely: benzoyl chloride was added at the start of the reaction to limit the growth of the polymer chain and as a stopper at the end of the reaction.

The method of the manufacture of thin birefringent films (TBF) was originally developed for lyotropic chromonic liquid crystals (LCLC). This is a multi-stage process which involves three successive steps of ordering during the film formation. To start with, the lyotropic liquid-crystalline state is achieved by making the proper concentration of the solution. The polarised optical microscopy (POM) image of a nematic liquid crystal formed by aqueous solution of the caesium salt of pQpdSS is presented in Figure 2(a).

In the second stage, the lyotropic liquid crystal is deposited under the action of a shear force onto a substrate, so that the shear force direction determines one of the principal axes in the resulting solid crystalline film. Thus, this shear force assisted directional deposition results in the macroscopically aligned structure on the substrate surface. The last step is drying and crystallisation which converts the lyotropic liquid crystal into a solid birefringent film.

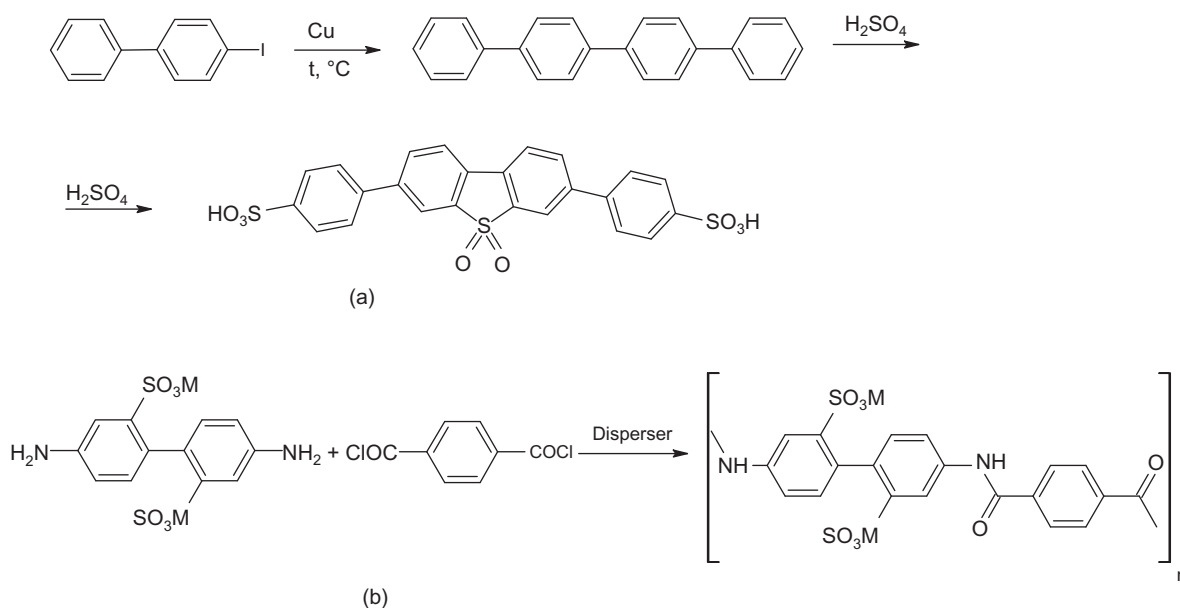For the first time, the technique was set to coat LCLC solutions of dichroic dyes for producing



Figure 1. Schemes of synthesis of (a) 4,4′-(5,5-dioxidodibenzo[b,d]thiene-3,7-diyl)dibenzenesulphonic acid and (b) poly(2,2′-disulphobenzidine terephthalamide).
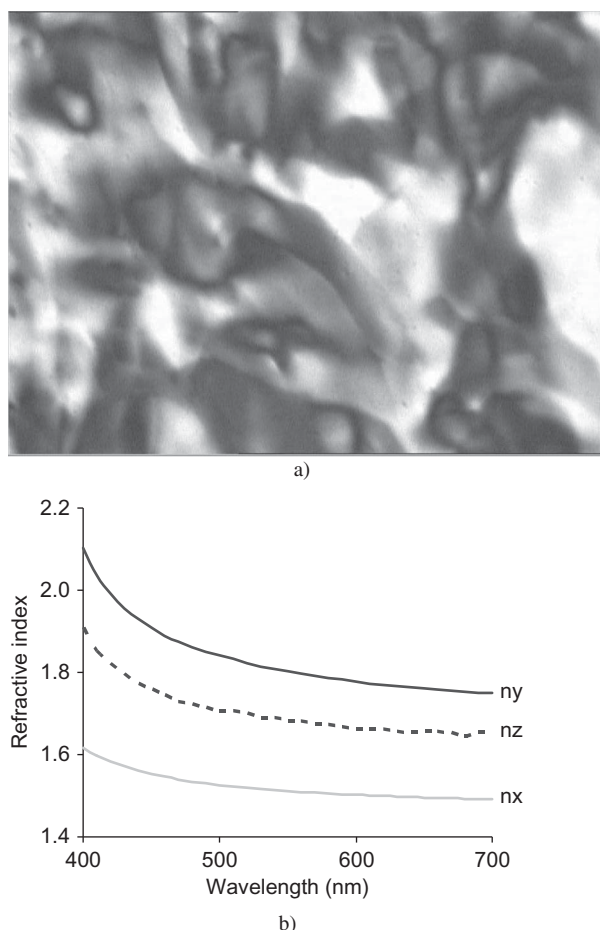
Figure 2. (a) POM image of lyotropic liquid crystalline solution formed by pQpdSS (caesium salt, $c = 15$ wt%) and (b) spectral dependence of the principal refractive indices for TBF prepared from the same solution.

polarising coatings [17]. It was further applied to colourless materials to prepare retardation films with negative optical anisotropy [18].

In this paper we expand the assortment of substances subjected to coating and introduce lyotropic liquid crystalline polymers (LLCPs) as a new class of lyotropic mesogens capable of forming thin birefringent films. The type of optical films produced by coating the conventional chromonic LLC is determined by negative optical anisotropy of the chromonic nematic phase and restricted with the range from negative A-plate to biaxial $B_A$-plate (see Table 1).

On the contrary, the nematic phase based on the main chain polymer is characterised by positive optical anisotropy, which opens up new possibilities for expanding the range of produced retarders. The following criteria can be formulated for the polymer:

(i) being water soluble;

(ii) having a rigid-rod main chain to form nematic LLC; and

(iii) having a main chain conjugated enough to provide proper optical anisotropy.

Rigid-rod polymers with a highly conjugated main chain generally show poor water solubility. For example, Kevlar [poly-(1,4-diaminophenylene terephthalamide)], one of the completely rigid-rod polymers with a highly conjugated main chain, is soluble in concentrated sulphuric acid and can form a lyotropic liquid crystal [26]. Poly(2,2′-disulphobenzidine terephthalamide) (PBDT) has a Kevlar-like rigid conjugated chain, but numerous sulphonic groups provide it with high water solubility [25]. PBDT can form a nematic phase which, however, exists in the lower concentration range and with longer inter-rod spacing than one would expect based on its rigidity [27]. The authors explain these phenomena with the strong electrostatic repulsive force yielded by the many anionic sites. The effects of temperature and electrolyte on the self-assembling properties of the sodium salt of PBDT in aqueous solutions were investigated [27, 28]. The POM image of a nematic liquid crystal formed by aqueous solution of caesium salt of PBDT is presented in Figure 3(a). Below we show, using the example of PBDT, that the water-soluble rigid-rod polymers can also be used to create thin birefringent films.

The process of manufacturing macroscopically ordered coatings from LLCP is performed in the same manner as coating of conventional chromonic LLC and involves the same principal points:

(i) preparation of LLC of the proper concentration;

(ii) aligning LLC by means of a shear force in the course of deposition onto a substrate; and

(iii) drying the film to fix a microscopically ordered structure.

## 3. Retarders made of individual compounds of pQpdSS and PBDT

### 3.1 Classification of retarders

The class of retardation films discussed in this paper is characterised by three principal axes (*a*, *b* and *c*), two of which (*a* and *b*) belong to the film plane, while the third (*c*) is oriented along the film normal. Without losing the generality the *a*-axis can be chosen along the principal in-plane direction corresponding to a lowest value of the in-plane refractive index $n_a$. The laboratory *xyz* frame is defined in a way. The *z*-axis is normal to the film and coincides with the principal *c*-axis, while the *x*-axis is along the coating direction

Table 1. Comparison of the proposed and existing retarder classifications.

| Existing designation | Proposed designation (equivalent names) | Optical axes orientation | Relation between principal refractive indices | NZ-factor |
|---|---|---|---|---|
| −A | −A | Single in-plane optical axis | $n_a < n_b = n_c$ | NZ = 0 |
| No name | +B$_A$ or −A$_B$ | Two optical axes are in the *ab*-plane that is the film plane. | $n_b > n_c > n_a$ | 0 < NZ < 1 |
| +A | +A | Single in-plane optical axis | $n_b > n_a = n_c$ | NZ = 1 |
| No name | +B$_C$ or −C$_B$ (+A$_C$; −C$_A$)$^{(*)}$ | Two optical axes are in *bc*-plane orthogonal to the film plane. | $n_b > n_a > n_c$ | NZ > 1 |
| −C | −C | Single optical axis is along the Eigen *c*-axis. | $n_a = n_b > n_c$ | +Infinity |
| +C | +C | Single optical axis is along the Eigen *c*-axis. | $n_a = n_b < n_c$ | -Infinity |
| No name | +C$_A$ or −A$_C$ (+C$_B$; −B$_C$)$^{(*)}$ | Two optical axes are in *ac*-plane orthogonal to the film plane. | $n_c > n_b > n_a$ | NZ < 0 |
| O plate | O plate$^{(**)}$ | The plane of the two principal *a*- and *b*-axes does not coincide with the film plane. | Any | No meaning |

Notes:*In general cases, the choice for in-plane *a*- and *b*- axes is optional, so if we allow the *a*-axis for the largest in-plane refractive index, then equivalent names appear. **The refractive index ellipsoid of an arbitrary O-plate can be transferred to one of the basic type listed in the table by a rotation procedure. Thus a more detailed classification of O-plates is possible on the basis of the defined types and simplest rotation making the two principal axes being parallel to the film plane.

that also coincides with one of the principal *a* or *b* axes; this depends on either the lowest or highest in-plane refractive index corresponding to the coating direction.

We classify the retardation films in terms of orientation of their optical axes and magnitudes of the principal refractive indices. In case of $n_b > n_c > n_a$, the two optical axes belong to the *ab* film plane. Such retardation films are named as A$_B$- or B$_A$-plates. In another case, when the two optical axes belong to the *ca* (*cb*) plane perpendicular to the film plane ($n_c > n_b > n_a$ or $n_b > n_a > n_c$), the retardation films are called C$_A$ (C$_B$) or A$_C$ (B$_C$) plates. Formally, the plates are defined as negative or positive depending on the sign of the difference of the principal refractive indices corresponding to the axes named by the capital letters. For instance, the C$_A$-plate is negative if $n_c - n_a < 0$. The negative C$_A$-plate is equivalent to the positive A$_C$-plate because $n_a - n_c > 0$. By analogy, the positive B$_A$-plate retarder is equivalent to negative A$_B$-plate. In degenerative cases, when there is only single optical axis, the designations A$_B$ and C$_A$ are reduced to the A and C, respectively. Thus the optical axis is along A or C direction for A or C plates, respectively.

The biaxiality of a birefringent film can be numerically expressed by a value of an NZ-factor (the ratio of out-of-plane retardation to in-plane retardation) that is calculated as:

$$NZ = \frac{R_{bc}}{R_{ba}} = \frac{\Delta n_{bc}}{\Delta n_{ba}} \equiv \frac{n_b - n_c}{n_b - n_a}, \quad (1)$$

where $R_{bc} = \Delta n_{bc} \cdot d$ and $\Delta n_{bc}$ are out-of-plane retardation and birefringence, and $R_{ba} = \Delta n_{ba} \cdot d$ and $\Delta n_{ba}$ are in-plane retardation and birefringence, respectively, and *d* is the thickness of the retardation film.

The generally accepted classification exists only for uniaxial retarders and includes positive/negative A-, C- and O-type retarders. We suggest a new classification of retarders based on the orientation of two optical axes with respect to the film plane. We believe that it is useful as a compatible classification with the existing retarder designations and a simple extension for the biaxial case. In Table 1 we compare the features of the classification known from the prior art and classification of the retarders proposed by the authors.

### 3.2 *Retarders from PQpdSS and PBDT*

The molecule of pQpdSS was designed in order to obtain a lyotropic liquid crystal phase capable of forming a biaxial retardation layer of B$_A$-type when
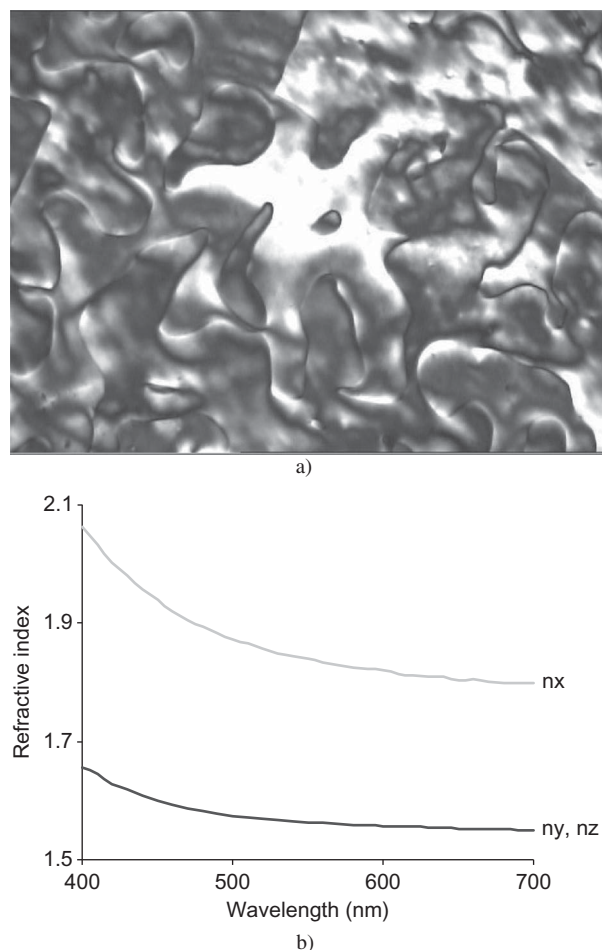
Figure 3. (a) POM image of lyotropic liquid crystalline solution formed by PBDT (caesium salt, $c = 6$ wt%) and (b) spectral dependence of principal refractive indices of TBF prepared from the same solution.

deposited onto a substrate. The conjugated hydrocarbon core is of plank-like shape providing different molecular polarisability in the three principal directions. Two sulphonic groups make for water solubility and impart amphiphilic properties to the molecule.

The NZ-factor of the produced $B_A$-plate retardation film at a wavelength of $\lambda = 550$ nm equals 0.4. The principal *a*-axis of the lowest value of the refractive index corresponds to the coating *x*-direction (Figure 2(b)).

Contrary to the pQpdSS, in case of PBDT the coating direction corresponds to the highest value of the refractive index $n_x \equiv n_b$, which also coincides with the unique optical axis. Thus the principal refractive indices of TBF produced from PBDT liquid crystalline solution obey the condition: $n_x > n_z = n_y$ which corresponds to the uniaxial positive A-plate retardation film (Figure 3(b)). Such a relationship between the principal refractive indices indicates that molecules in

the films are oriented with their long axes preferably parallel to the coating direction. The NZ-factor of positive A-plate retardation film equals 1.

## 4. Guest–host (PBDT-pQpdSS) system for retarders with controlled properties

### 4.1 Optical anisotropy control

The guest–host system based on pQpdSS and PBDT is the focus of the present paper. As shown above, separately the components are capable of forming lyotropic nematic phase at proper concentrations and can be used to prepare the retardation films with fixed optical anisotropy. In case of pQpdSS, the nematic LLC phase is based on biaxial plank-like supramolecules, whereas the nematic phase of PBDT is formed by rod-like polymer macromolecules.

The ratio of the two compounds varies over a wide range, and consequently the terminology distinguishing the guest and host type molecules is quite conditional. In the present paper we consider pQpdSS as the host molecules, independent of the concentration. When both the water solutions are mixed, we get guest–host nematic LLC with the axes of PBDT macromolecules being preferably parallel to the axes of pQpdSS molecular stacks. Guest–host LLCs show shear-thinning behaviour typical of nematic liquid crystals (Figure 4). The process of deposition of the guest–host LLC onto a substrate is ruled by the same principles described for the individual components, resulting in formation of the guest–host solid anisotropic film with one of the principal axes along the coating direction (Figure 5).

The control of principal refractive indices of the guest–host system is based on a superposition of guest
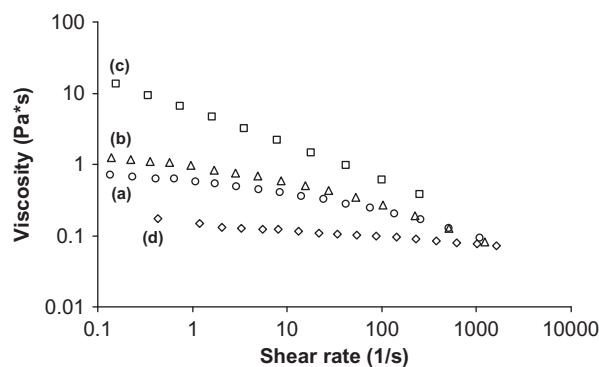


Figure 4. Viscosity vs. shear rate: (a) pure pQpdSS, 10.7 wt%; (b) guest–host system having weight ratio PBDT:pQpdSS = 17:83, 16.2 solid wt%, PBDT $M_n = 25,000$; (c) guest–host system having weight ratio PBDT:pQpdSS = 64:36, 7.3 solid wt%, PBDT $M_n = 145,000$; (d) pure PBDT, 20 wt%, $M_n = 25,000$.
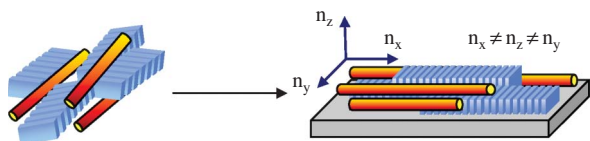
Figure 5. Scheme of assumed mutual position of kinetic units of PBDT and pQpdSS in bulk LLC solution and after deposition onto a substrate.

and host macroscopic polarisability tensors characterised by coinciding principal axes but different Eigen (principal) values. In the frame of the superposition principle, the principal components of the polarisability tensor for the guest-host film are expressed as follows:

$$\chi_i = v_h\chi_{h,i} + v_g\chi_{g,i} \equiv v_h\chi_{h,i} + (1-v_h)\,\chi_{g,i}, i \tag{2}$$
$$\in \{x,y,z\},$$

where $v_h$, $v_g$ are volume fractions occupied by host and guest molecules in the whole volume of the guest-host system ($v_h + v_g = 1$), respectively, and $\chi_{h,i}$, $\chi_{g,i}$ are the principal values of the polarisability tensors of the films prepared from individual host and guest components, respectively. Below, the subscripts '$h$' and '$g$' are attributed to the host (pQpdSS) and guest (PBDT) material, respectively. Taking into account that, for the non-magnetic materials, there is an explicit relationship between the principal values of the polarisability and refractive indices ($n_i = \sqrt{1+\chi_i}$), from Equation (2) it is easy to obtain:

$$n_i = \sqrt{n_{g,i}^2 + v_h\left(n_{h,i}^2 - n_{g,i}^2\right)}$$
$$\equiv n_{g,i}\sqrt{1 + v_h\frac{\delta n_i}{n_{g,i}}\left(2 + \frac{\delta n_i}{n_{g,i}}\right)}, \tag{3}$$

where $n_{h,i}$, $n_{g,i}$ are the principal refractive indices of the films made exclusively of the host and guest materials, respectively, and $\delta n_i = (n_{h,i} - n_{g,i})$. If $\delta n_i/n_{g,i} << 1$, then expanding Equation (3) in series and leaving the first order terms, Equation (3) is reduced to an approximate expression:

$$n_i \cong n_{g,i} + v_h\delta n_i \equiv v_h n_{h,i} + (1-v_h)n_{g,i} \tag{4}$$

According to Equation (4), at a small relative difference ($\delta n_i/n_{g,i}$) of the refractive indices for the host and guest compounds, the principle of the superposition (Equation (2)) can also be approximately applied directly to the principal refractive indices. In our case $\delta n_i/n_{g,i} \sim 0.15$ and use of Equation (4) instead of

Equation (3) is justified within a relative inaccuracy of about 1% ($(\delta n_i/n_{g,i})^2/2 \sim 0.01$ for all the volume fractions). However, it is important to emphasise that, in the general case, the even more accurate Equation (3) which gives the concentration dependence in terms of the squares of the refractive indices should be used with caution because the basic superposition principle expressed by Equation (2) is an approximation. It can only be used if the intermolecular interactions are weak or if the molecular fields acting in the guest–host system are very similar to those in the films of the individual components. Fortunately, the experimental data confirm that the superposition principle works quite well in our case.

If the densities of the mixed materials are close to each other, then Equation (4) can be further simplified to one convenient for practical usage:

$$n_i \approx c \cdot n_{h,i} + (1-c) \cdot n_{g,i}, \tag{5}$$

where $c$ is the weight concentration of the host biaxial component in the guest–host system.

As stated above, the coating direction corresponds to the minimal and maximal principal values of the dielectric tensor for the host material (pQpdSS) and guest material (PBDT), respectively. Thus in the guest–host film the refractive indices depend on the concentration of the host molecules, and at a certain concentration $c = c^*$ of the host component, $n_x = n_y$; so, in a general case, we have either the isotropic (if $n_x = n_y = n_z$) or uniaxial (if $n_x = n_y \neq n_z$) C-type plate. It is quite important that at $c > c^*$ and $c < c^*$ we get $A_B$ and $A_C$ plates, respectively, which are very different in the sense of the orientation of their two optical axes. It follows from Equation (5) that the value $c^*$ can be expressed in terms of the in-plane anisotropy of the films made of the guest and host compounds as follows:

$$c^* = \frac{n_{g,x} - n_{g,y}}{(n_{g,x} - n_{g,y}) - (n_{h,x} - n_{h,y})}$$
$$\equiv \frac{\Delta n_{g,xy}}{\Delta n_{g,xy} - \Delta n_{h,xy}}. \tag{6}$$

Then, from Equations (1) and (5) on account of the uniaxiality of the film made of the guest compound ($\Delta n_{g,yz} = 0$), the NZ-factor of the guest–host film can be calculated as:

$$\left[\begin{array}{l} NZ = \dfrac{c \cdot \Delta n_{h,xz} + (1-c) \cdot \Delta n_{g,xz}}{c \cdot \Delta n_{h,xy} + (1-c) \cdot \Delta n_{g,xy}}, if\ \ 0 \le c < c^* \\[3mm] NZ = \dfrac{c \cdot \Delta n_{h,yz}}{c \cdot \Delta n_{h,yx} + (1-c) \cdot \Delta n_{g,yx}}, if\ \ c^* < c \le 1. \end{array}\right. \tag{7}$$

Particularly, for the wavelength of 550 nm, the refractive indices of the films of the individual compounds take the values: $n_{h,x} = 1.51$, $n_{h,y} = 1.84$, $n_{h,z} = 1.71$, $n_{g,x} = 1.83$, and $n_{g,y} = n_{g,z} = 1.56$. Consequently, Equations (7) are reduced to the following expressions, which are quite useful for practical evaluation of the NZ-factor of a particular guest–host system:

$$\left[ \begin{array}{l} NZ = \dfrac{1 - 1.74c}{1 - 2.22c}, \text{if } 0 \le c < 0.45 \\[2mm] NZ = \dfrac{4.62c}{1 - 0.45c}, \text{if } 0.45 < c \le 1. \end{array} \right. \tag{8}$$

Mixtures with several different ratios of pQpdSS to PBDT were investigated. The experimental dependence of the NZ-factor of composite films on the weight portion of pQpdSS in the liquid crystalline solution is presented in Figure 6. Experimental data are in good agreement with values calculated using Equation (8). One can see that the NZ-factor can be tuned in a wide range. The low limit is defined by the NZ-factor of individual $B_A$ films made of the host compound. At the same time, this limit of the achievable NZ-factor can be further reduced to any desirable value down to zero by adding a third component capable to form a uniaxial negative A-plate film.

We would also like to point out that the spectral dispersion of the film birefringence can also be controlled efficiently. This is an especially important feature for applications. Indeed, despite the individual g- and h-materials showing strong spectral dispersion of the principal refractive indices, the resultant spectral dependence of the retardation provided by the composite film can be negligible or even inversed (anomalous dispersion). This is because in the mixture the system of rod-like polymer molecules performs as a positive A-type material, while the columnar supramolecules perform as negative material. Thus, the effect of compensation by the spectral dispersion for the birefringence is observed. The
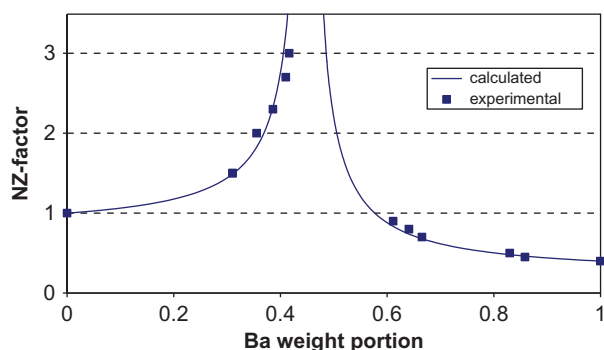


Figure 6.  NZ-factor of the solid retardation film vs. weight portion of biaxial $B_A$-plate component (pQpdSS) in the liquid crystalline solution.

principal axis of highest refraction index and highest dispersion of the polymer material coincides with the axis of the lowest refractive index and lowest dispersion of the supramolecules, and *vice versa* (the axes of highest refractive indices with strong dispersion of the supramolecules correspond to the lowest dispersion of the polymer). Thus in A-composite material we equalise the spectral dispersion for the two principal refractive indices, and as a result the dispersion for the birefringence is reduced. By controlling a difference between spectral dependencies of the principal refractive indices with strong dispersion for the individual g- and h-materials, one can efficiently control the resultant dispersion of birefringence.

## 4.2   Environmental stability and mechanical properties

For the majority of display applications, the retarders should possess high environmental stability in order to resist destructive processes caused by water which can permeate through porous polymeric films and adhesives. The industrial requirement on environmental stability is the ability to pass a 1000 hours' test at a temperature of 60°C and a relative air humidity of 90% without significant change of the retardation and haze properties.

Since thin birefringent films are produced from water-soluble materials, an additional treatment should be applied to the films. The developed procedure comprises treatment of the solid films with an aqueous solution of a barium salt (e.g. barium nitrate), which results in water-insoluble salts of pQpdSS and PBDT.

Besides control of the refractive indices, use of the guest–host systems described allows the mechanical properties to be corrected. For instance, the films exclusively based on pQpdSS tend to generate cracking during a certain treatment such as conversion to water-insoluble form. Adding PBDT enhances the mechanical strength of the films and prevents the cracking. The effect is achieved at minimal share of polymeric additive of ~15 wt%.

Investigation of various lyotropic chromonic liquid crystals using wide-angle X-ray scattering (WAXS) showed that the interplanar spacing within the molecular stack is equal to ~3.4 Å [29, 30]. This value was further confirmed for solid films [31]. Using these data, we can estimate that a length of the monomeric unit of PBDT is ~18 Å, corresponding to ~5.3 molecules of pQpdSS in the stack. Thus the weight ratio close to 15:85 corresponds to a condition when each stack of pQpdSS is interlaced with the PBDT macromolecule. The experimental results are in good agreement with

the calculated guest–host weight ratio 15:85, when one row of pQpdSS stacks is alternated by one PBDT polymeric chain.

### 4.3  Thermal stability

Typical polymer stretched retarders are stable up to 80°C. At higher temperatures, degradation of the mechanical and optical properties occurs. On the other hand, the thin birefringent films are stable up to 230–250°C. In addition, the physical thickness of the TBFs is 50–100 times lower compared with the conventional stretched films. These properties open up the possibility of using them as in-cell retarders. In-cell application implies that a retardation film is printed onto the inner surface of one of the LCD panel substrates in sequence with other functional layers such as colour filters, masks and polyimide alignment layers. The arrangement of a retarder inside the LCD cell eliminates the risk of delamination, bubbling or involving particles from outside (typical defects for external optical films). In this sense, cells with in-cell retarders show higher durability compared with the cells with external plastic retarders. This is especially important for LCDs working in harsh environmental conditions.

To simulate the high-temperature stages of LCD production process (such as polyimide curing and cell sealing), a temperature test including several repeating stages was performed.

Films coated onto display glass and converted into a water-insoluble form were placed in an oven and heated to 230°C in air. After one hour, the samples were cooled to room temperature and then, after interim measurements were taken, heated to the same temperature for an additional two hours. The experiments show that degradation of the samples does not occur: the transmittance and haze did not change. The optical anisotropy of the films slightly increased; it reached a maximum value within the first hour of heating and then did not change with further treatment. The change of the optical anisotropy may be associated with an increase in the ordering of the molecules in TBF during the high temperature treatment. A similar effect was observed earlier for TBF comprising pQpdSS as a single birefringent component [32, 33].

The results of thermal stability tests show that $B_A$ and $A_C$-plate retarders based on pQpdSS and PBDT guest–host films meet the requirements for in-cell applications.

### 5.  Optical applications

The retardation films prepared with the guest–host LLC mixture are efficient for LCD viewing angle enhancement. The two most widely spread LCD modes for TV applications are VA mode and IPS mode. In the sense of optical compensation, the VA mode LC cell in the black state is a positive C-plate while the IPS mode LC cell is a positive A-plate. Thus, the negative C-type retarder is required to compensate, for instance, the LC layer in VA LCD. Besides the compensation of LC layer an additional $B_A$-plate is required to suppress light leakage through the polarisers. The $B_A$-plate retarder is also very effective for optical compensation of the IPS mode LCDs.

Figure 7(a) demonstrates the dependences of principal refractive indices on wavelength for the films produced from guest–host material with a weight ratio PBDT:pQpdSS = 17:83. The refractive indices of the film satisfy the condition $n_x < n_z < n_y$, which corresponds to biaxial $B_A$-plate. The NZ-factor at a wavelength of 550 nm equals 0.5. The two retarders (negative C and $B_A$-plate) mentioned for VA mode LCD compensation can be replaced with single $A_C$-plate TBF [30]. Figure 7(b) shows the dependence of principal refractive indices on wavelength for the film produced from a mixture with the weight ratio PBDT:pQpdSS = 59:41. The refractive indices of the film satisfy the condition $n_x > n_y > n_z$, which corresponds to biaxial $A_C$-plate. The NZ-factor at a wavelength of 550 nm equals 2.7.

The simulation results of the viewing angle LCD performance are illustrated in Figure 8. The prototype of VA mode LCD compensated with coated retardation films was described earlier [32]. The contrast ratio at viewing angles of 60° with respect to the normal was 20 times higher than that for the non-compensated cell and exceeded a value of 100 [34].

As already mentioned, IPS mode LCD compensation can be performed using a single $B_A$ plate TBF [33]. Viewing angle performance simulation results are shown in Figure 9.

### 6.  Conclusions

We have proposed a new approach for the development of lyotropic liquid crystal functional materials for optical applications. The developed 'guest–host' approach is based on the molecular design and mixing of two quite different types of compounds:

(i)  lyotropic LC based on columnar supramolecules; and
(ii)  water soluble rod-like polymer molecules.

The developed materials allow the production of optical retardation films which have tunable optical anisotropy. In particular, these materials allow the creation of a large assortment of thin film biaxial optical retarders with desirable values for their principal refractive indices. They extend the set of retarders that
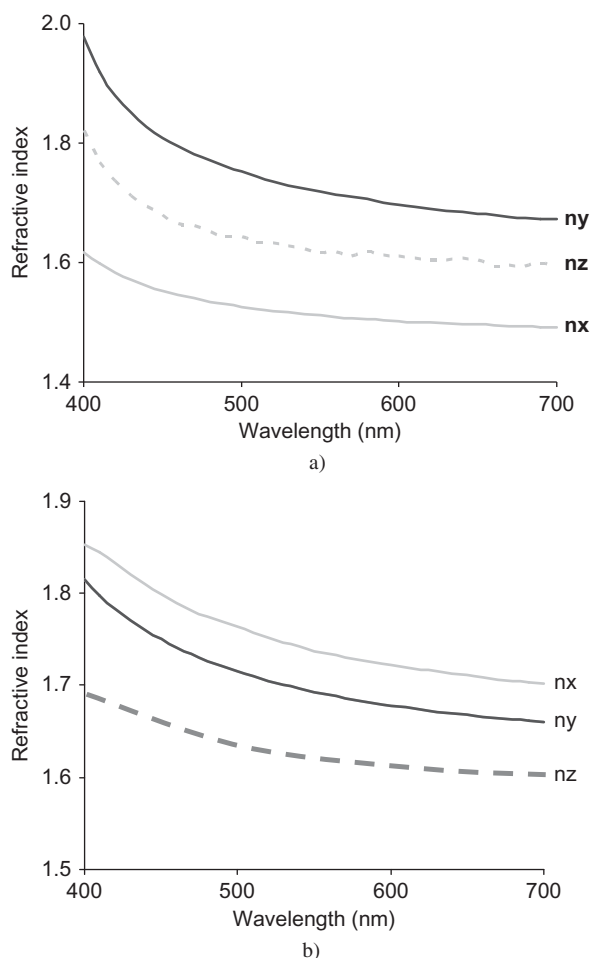
Figure 7. Principal refractive indices spectral dependence for thin birefringent films produced from pQpdSS-PBDT LLC solutions: (a) weight ratio pQpdSS:PBDT = 83:17; and (b) weight ratio pQpdSS:PBDT = 41:59.
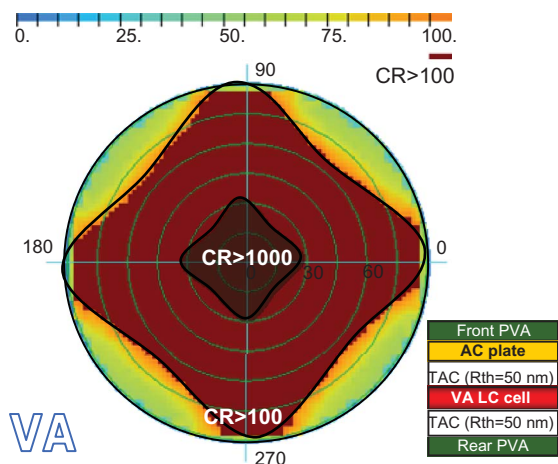


Figure 8. Scheme and simulation results of multidomain VA LCD viewing angle contrast ratio (CR).
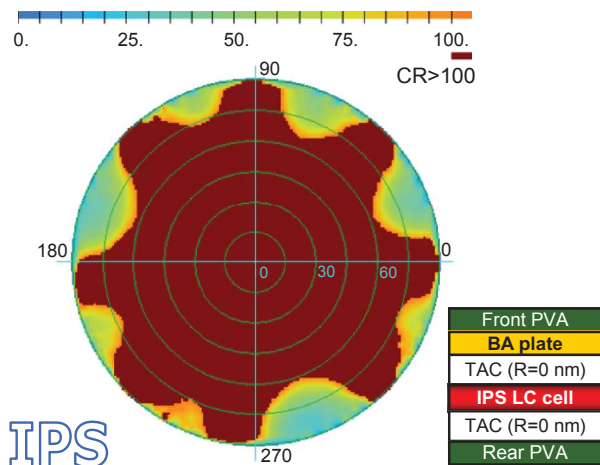


Figure 9. Scheme and simulation results of multidomain IPS LCD viewing angle contrast ratio (CR).

can be manufactured by the LLC coating technique. Such retarders can be used in modern LCDs and TVs for optical compensation and enhancement of their performance. The guest–host coatable retarders also possess improved mechanical properties, and environmental and thermal stability.

## 7.    Experimental

### 7.1.1    Synthesis of 4,4'-(5,5-dioxidodibenzo[b,d] thiene-3,7-diyl)dibenzenesulphonic acid

Ground 4-iodobiphenyl (5.6 g, 0.020 mol) was mixed thoroughly with 7 g of copper (45 µm powder). The mixture was placed in a Teflon-lined bomb, heated to 270°C and held at temperature for 1 h. The product of the reaction was then recrystallised from *N*-methylpyrrolidone. The yield of *p*-quaterphenyl was 2 g (0.007 mol). *p*-Quaterphenyl (2 g) was sulphonated with 55 g of sulphuric acid monohydrate at 80°C, then the reaction mass was cooled, quenched with 14 ml of water and filtered. The resulting filter cake was washed with 160 ml of glacial acetic acid, then squeezed and dried at 130°C. The yield of 4,4'-(5,5-dioxidodibenzo[b,d]thiene-3,7-diyl)dibenzenesulphonic
acid was 1.3 g (0.0025 mol).

^{1}H NMR (D6-DMSO): $\delta$ 8.38–8.38 (m, 4H), 8.19 (dd, 2H, [4]$J$ = 1.37 Hz, [3]$J$ = 7.54 Hz, 2H[B]), 7.84 (d, 4H, [3]$J$ = 8.24 Hz), 7.73 (d, 4H, [3]$J$ = 8.24 Hz).

^{13}C NMR (D6-DMSO): $\delta$ 148.68, 142.64, 138.78, 133.25, 130.11, 126.97, 126.77, 123.93, 120.41.

### 7.1.2    Synthesis of poly(2,2'-disulpho-4,4'-benzidine terephthalamide) caesium salt

4,4'-Diaminobiphenyl-2,2'-disulphonic acid (1.377 g, 0.004 mol) was added to 140 ml of water with

agitation. A solution of 1.34 g (0.008 mol) CsOH·H$_2$O in 18 ml of water was added, followed by a solution of 1.43 g (0.004 mol) caesium carbonate in 18 ml of water. Dichloromethane (70 ml) was then added and the mixture was agitated with an ultra disperser at 8000 rpm. While stirring the obtained emulsion at high speed, a solution of 0.9 g (0.0044 mol) of terephthaloyl chloride and 0.07 ml of benzoyl chloride in 70 ml of dry dichloromethane was added. The mixture was agitated at 8000 rpm for 5 min and a solution of 0.7 ml of benzoyl chloride in 7.5 ml of dichloromethane was added to stop polymerisation of the reaction. The reaction mass was further agitated for 3 min, poured into 1 l of ethanol and stirred until a homogeneous mixture was obtained. The polymer was isolated by filtration, dissolved in 70 ml of water and precipitated on mixing with 280 ml of ethanol. The precipitate was isolated, dissolved in 70 ml of water and precipitation into ethanol was repeated. At the end, re-precipitation was done into 280 ml of acetone and the product was dried at 100°C. The yield of the polymer was 2.4 g. Gel permeation chromatography (GPC) analysis of the sample was performed with a Hewlett Packard 1050 high-performance liquid chromatography chromatograph with diode array detector ($\lambda$ = 230 nm) using Varian GPC software Cirrus 3.2 and a SHODEX Asahipak GF-7M HQ column with guard column Asahipak GF-1G. A mixture of acetonitrile and 0.05 M phosphate buffer (pH = 6.9 – 7.0) in the ratio 40/60, respectively was used as the mobile phase. The flow rate was 0.4 mL min$^{-1}$, the column temperature was 30°C. Samples of the poly (para-styrenesulphonic acid) sodium salts were used as the GPC standards. The final product is a mixture of the polymer (90%) and oligomer (10%) fractions. The number average molecular weight (Mn), weight average molecular weight (Mw) and poly dispersity (PD) of the polymer fraction were found to be 7.8 $\times$ 10$^4$, 17.4 $\times$ 10$^4$, and 2.2, respectively. The Mn, Mw and PD of the oligomer fraction were found to be 0.5 $\times$ 10$^4$, 0.7 $\times$ 10$^4$ and 1.4, respectively.

### 7.1.3   *Production of TBF from pQpdSS*
pQpdSS acid (1g) was mixed with 5.8 g of distilled water and 3.2 g of a 20% aqueous solution of caesium hydroxide, and then stirred at room temperature (23°C) for approximately 1 h until a lyotropic liquid crystal solution was formed. The liquid crystalline solution was applied onto a specially prepared glass plate surface with a Mayer rod #4 which was moved at a linear velocity of ~200 mm s$^{-1}$ at room temperature of 23°C and a relative humidity of 50%. The coated liquid layer of the solution was dried at the same humidity and temperature. The solid film was characterised with a physical thickness of ~400 nm.

### 7.1.4   *Production of TBF from PBDT*
PBDT caesium salt (1 g) was dissolved in 15.7 g of distilled water, and then stirred at room temperature (23°C) for approximately 1 h until a lyotropic liquid crystal solution was formed. The liquid crystalline solution was applied onto a specially prepared glass plate surface with a Mayer rod #4 which was moved at a linear velocity of ~200 mm s$^{-1}$ at room temperature of 23°C and a relative humidity of 50%. The coated liquid layer of the solution was dried at the same humidity and temperature. The dried film was characterised with physical thickness of ~180 nm.

### 7.1.5   *Production of TBF of guest–host film*
pQpdSS acid (1 g) was mixed with 4.06 g of distilled water and 3.2 g of a 20% aqueous solution of caesium hydroxide, and then stirred at room temperature (23°C) for approximately 1 h until a lyotropic liquid crystal solution was formed. Separately, 0.307 g of PBDT caesium salt was dissolved in 4 g of distilled water, and then stirred at room temperature (23°C) for approximately 1 h until a lyotropic liquid crystal solution was formed. The two LLC solutions were combined and the resulting mixture was additionally stirred at room temperature for approximately 10 h until a homogeneous liquid crystalline solution was formed. The solution was applied to a specially prepared glass plate surface with a Mayer rod #4 at a linear velocity of ~200 mm s$^{-1}$ at room temperature of 23°C and a relative humidity of 50%. The coated liquid layer of the solution was dried at the same humidity and temperature. The solid film was characterised with a physical thickness of ~500 nm.

This example describes the preparation of a lyotropic liquid crystal and film containing pQpdSS and PBDT in weight ratio 83:17. In the same way, the solutions and films were prepared with weight ratios 86:14, 67:33, 64:36, 61:39, 42:58, 41:60, 39:61, 36:64, and 31:69.

### 7.1.6   *LLC solutions viscosity vs. shear rate measurements*
Flow measurements were staged on a stress-controlled TA AR 550 rheometer. The 'cone-and-plate' geometry of the measuring unit was used. The cone diameter was 60 mm at a gap angle of 2°. Shear viscosity vs. shear rate/stress was measured in the steady-state flow regime. All measurements were performed at 30°C.

### 7.1.7 *Optical characterisation of thin birefringent films*

In order to determine the spectral dependence of the TBF principal refractive indices, a complex measurement and calculation procedure was performed. First, the transmittance and reflectance of the films coated onto a glass substrate were measured for the beam polarised along the coating direction. The polarised transmittance spectra were measured at normal incidence, while the reflectance measurements were performed at an incidence angle of 12° (S-polarised light) in a wavelength range of 400–700 nm using a Varian Cary-500 spectrophotometer. The obtained data were processed using specially designed software solving Maxwell equations on account of Kramers–Kronig relation [35, 36] in order to determine the spectra of in-plane principal refractive indices. Secondly, the phase retardation spectra were measured at different incidence angles of 0°, 30°, 45° and 60°. The spectra of the out-of-plane principal refractive indices were obtained from these measurements using the referenced software.

### Acknowledgements

### References

[1] Broer, D.J.; van Haaren, J.A.M.M.; van de Witte, P.; Bastiaansen, C. *Macromol. Symp.* **2000**, *154*, 1–13.

[2] Bahadur, B. In *Handbook of Liquid Crystals*; Demus, D., Goodby, J., Gray, G.W., Spiess, H.-W., Vill, V., Eds.; Wiley-VCH: Weinheim, 1998; Vol. 2A, pp 257–260.

[3] Anslyn, E.V.; Dougherty, D.A. *Modern Physical Organic Chemistry*; John Wiley: New York, 2006.

[4] Lodish, H.; Berk, A.; Kaiser, C. *Molecular Cell Biology*, 6th ed.; Freeman: New York, 2008.

[5] Bobrov, Y.; Kuchenkova, O.; Kouznetsov, M.; Lazarev, P.; Manko, A.; Nazarov, V.; Ovchinnikova, N.; Paukshto, M.; Protsenko, P.; Remizov, S. *J. SID* **2004**, *12/2*, 125–133.

[6] Mori, H. In *Proceedings of IDRC'06*, Kent, OH, Sept 18–21, 2006; Society for Information Display: Campbell, CA, 2006; pp 67–70.

[7] Satoh, T.; Arakawa, K.; Yamazaki, M. *EKISHO* **2005**, *9*, *4*, 47–53.

[8] Hirota, M.; Okude, S.; Hori, T.; Arakawa, K. In *Proceedings of IDW'06*, Otsu, Japan, Dec 6–8, 2006; Society for Information Display: Campbell, CA, 2006; pp 315–318.

[9] Nakayama, H.; Fukagawa, N.; Nishiura, Y.; Yasuda, T.; Ito, T.; Mihatashi, K. *J. Polym. Sci. Technol.* **2006**, *19*, 2, 169–173.

[10] Harding, R.; Parri, O.; Marden, S.; Skjonnemand, K.; Verrall, M.; Fiebranz, B. In *Proceedings of IDW'06*, Otsu, Japan, Dec 6–8, 2006; Society for Information Display: Campbell, CA, 2006; pp 307–310.

[11] Skjonnemard, K.; Parri, O.; Graham, D.G.; Perett, T. Negative Retardation Film. US Patent 7,477,343, January 13, 2009.

[12] Tilsch, M.K.; Hendrix, K.; Tan, K.; Shemo, D.; Bradley, R.; Erz, R.; Buth, J. *Thin Solid Films* **2007**, *516*, 107–113.

[13] Seiberle, H.; Benecke, C.; Bachels, T. *SID Symposium Digest* **2003**, *34*, 1162–1165.

[14] Oikawa, T.; Yasuda, S.; Takeuchi, K.; Sakai, E.; Mori, H. *J. SID* **2007**, *15/2*, 133–137.

[15] Seiberle, H.; Bachels, T.; Benecke, C.; Ibn-Elhaj, M. In *Proceedings of IDW'06*, Otsu, Japan, Dec 6–8, 2006; Society for Information Display: Campbell, CA, 2006; pp 33–306.

[16] Hasebe, H.; Kuwana, Y.; Nakata, H.; Yamazaki, O.; Takeuchi, K.; Tsai, J.-C. *SID Symposium Digest* **2008**, *39*, 1904–1907.

[17] Bobrov, Y.; Cobb, C.; Lazarev, P.; Bos, P.; Bryand, D.; Wonderly, H. *SID Symposium Digest* **2000**, *31*, pp 1102–1107.

[18] Lazarev, P.; Paukshto, M. In *Proceedings of IDW'00*, San Jose, CA, Nov 29–Dec 1, 2000; Society for Information Display: Campbell, CA, 2000; pp 1159–1160.

[19] Lydon, J. In *Handbook of Liquid Crystals*: Demus, D., Goodby, J., Gray, G.W., Spiess, H.-W., Vill, V., Eds.; Wiley-VCH: Weinheim, 1998; Vol. 2B, pp 981–1007.

[20] Yip, W.C.; Kwok, H.S.; Kozenkov, V.M.; Chigrinov, V.G. *Displays* **2001**, *22*, 27–32.

[21] Palto, S.P.; Remizov, S.; Kasianova, I.; Guselnikov, N.; Lazarev, A. In *Proceedings of IDW'06*, Otsu, Japan, Dec 6–8, 2006; Society for Information Display: Campbell, CA, 2006; pp 311–314.

[22] Palto, S.; Kasianova, I.; Kharatiyan, E.; Kuzmin, V.; Lazarev, A.; Lazarev, P. *SID Symposium Digest* **2007**, *38*, 1563–1566.

[23] Ullmann, F.; Neyer, G.M.; Loewental, O.; Gilli, E. *Justus Liebigs Ann. Chem.* **1904**, *332*, 38–81.

[24] Fanta, P.E. *Chem. Rev.* **1964**, *64*, 613–632.

[25] Sarkar, N.; Kershner, L.D. *J. Appl. Polym. Sci.* **1996**, *62*, 393–408.

[26] Zhou, M.; Frydman, V.; Frydman, L. *J. Phys. Chem.* **1996**, *100*, 19280–19288.

[27] Funaki, T.; Kaneko, T.; Yamaoka, K.; Ohsedo, Y.; Gong, J.P.; Osada, Y.; Shibasaki, Y.; Ueda, M. *Langmuir* **2004**, *20*, 6518–6520.

[28] Yang, W.; Furukawa, H.; Shigekura, Y.; Shikinaka, K.; Osada, Y.; Gong, J.P. *Macromolecules* **2008**, *41*, 1791–1799.

[29] Edwards, D.J.; Ormerod, A.P.; Tiddy, G.J.T.; Jaber, A.A.; Mahendrisingham, A. In *Physico-Chemical*

*Principles of Color Chemistry*; Advances in Color Chemistry series, 1996; Vol. 4, pp 83–106.

[30] Dembo, A.; Ionov, A.; Lazarev, P.; Manko, A.; Nazarov, V. *Molecular Materials* **2001**, *14*, 275–290.

[31] Lazarev, P.; Lokshin, K.; Nazarov, V. *Molecular Materials* **2001**, *14*, 303–311.

[32] Lazarev, A.; Geivandov, A.; Kharatiyan, E.; Lazarev, P.; Yurchenko, D. *SID Symposium Digest* **2008**, *39*, 1894–1896.

[33] Lazarev, A.; Geivandov, A.; Kasianova, I.; Kharatiyan, E.; Lazarev, P.; Palto, S. In *Proceedings of IDW'08*, Niigata, Japan, 2008; Society for Information Display: Campbell, CA, 2008; pp 1741–1744.

[34] Geivandov, A.; Kasianova, I.; Kharatiyan, E.; Lazarev, A.; Lazarev, P.; Palto, S. In *Proceedings of IDW'07*, Sapporo, Japan, Dec 5–7, 2007; Society for Information Display: Campbell, CA, 2007; pp 2057–2060.

[35] Sheik-Bahae, M. In *Encyclopedia of Modern Optics:* Guenther, R.D., Ed.; Academic Press: Amsterdam, 2005.

[36] Palto, S.P. *JETP* **2001**, *92*, 552–560.